Frequency limits of 1/*f* noise

2000 J. Phys.: Condens. Matter 12 2469

(http://iopscience.iop.org/0953-8984/12/11/313)

J. Phys.: Condens. Matter **12** (2000) 2469–2483. Printed in the UK PII: S0953-8984(00)08907-4

Frequency limits of $1/f$ noise

Joseph F Stephany
Lakeston Research Center, PO Box 586, Webster, NY 14580, USA

Received 25 October 1999, in final form 11 January 2000

Abstract. The concept that universal $1/f$ noise is caused by defect migration is shown to be supported by experimental results and further theoretical development. Migrating defects are bombarded by conduction electrons and are driven against adjacent lattice atoms forming an impacted mass. It is predicted that a time constant, τ_s, defined as the average time taken for a single non-impacted defect to impact against an adjacent atom, would consequently vary with the externally applied current, I_0. This would then, in turn, cause the high-frequency cut-off point of $1/f$ noise, $f_s = \tau_s^{-1}$, to vary with I_0. For the case of a carbon conductor not only was this observation experimentally verified but also numerous new properties of $1/f$ noise were discovered. Among these were the following. (1) The curve of f_s versus I_0 exhibited resonances. (2) It was found that the more rigid the lattice was the closer the noise was to an exact $1/f$ response with a value fitting the Hooge empirical formula. (3) The noise spectrum above f_s was found to behave as $f^{2(\kappa-1)}$ with an attenuating parameter $\kappa = I_\kappa/(I_0 + I_\kappa)$ where $I_\kappa^2 R_0$ is the thermal energy flowing in the direction of the current as given by the Stefan–Boltzmann law. (4) A zero-current ($I_0 = 0$) noise source was found with an amplitude given by $S(\omega) = \sqrt{m_-/m_+}(I_\kappa^2/N_0) f^{-1}$. (5) A definite low-frequency end to the observable $1/f$ dependence was also found as indicated by a change from a $1/f$ to a $1/f^2$ frequency dependence as predicted by the theory.

1. Introduction

There is a large body of evidence showing that universal $1/f$ noise is caused by defect migration [1–21]. The term 'universal $1/f$ noise' is taken here to mean the $1/f$ noise observed in all metallic conductors and semiconductors that is generated by the same mechanism, but is not intended to mean all possible forms of $1/f$ noise that are observed. A previously published theory of the origin of $1/f$ noise [22, 23] was based on the concept that a theory of $1/f$ noise could be formulated from a viewpoint not significantly different from that used for the explanation of generation–recombination noise or thermal noise. It was shown that defects of any kind, including defects created by thermal fluctuations, influence the initial velocity of conduction electrons after a lattice collision in a manner that creates $1/f$ noise. Experiments designed to verify this theory resulted in the discovery of numerous characteristics of $1/f$ noise that apparently have not been reported previously. The explanation of these observations required further development of the original theory.

Using the elementary model proposed, the high-frequency cut-off of the spectral density of $1/f$ noise was theoretically found to be dependent on a parameter τ_s which is a time constant that is defined as the average time that it takes bombarding conduction electrons to move a single non-impacted lattice defect to a position of impact against an adjacent neighbour atom. After this first impact the time interval required increases as the number of impacted atoms builds up. The reciprocal of τ_s is the frequency f_s, which is the upper limit of the $1/f$ noise spectrum at which the frequency dependence of this mechanism changes to another dependence. Since

0953-8984/00/112469+15$30.00

τ_s is field dependent, f_s would vary with the applied field. Finding this variation was a major step in verifying the theory, or, at least, showing that this prediction of the theory is borne out experimentally.

2. Experimental methods

It is first necessary to obtain samples that exhibit a high-frequency cut-off of the $1/f$ dependence at a point above the thermal noise. This is difficult for metallic conductors since $1/f$ noise is often of low amplitude due to the high values of N_0, placing the high-frequency cut-off of the $1/f$ response at a point where it is less than the thermal noise. Increasing the current to increase the observed noise results in excessive sample heating making the results questionable. Although this characteristic response was observed experimentally in older types of carbon composition resistors some time ago, where f_s was definitely observed to vary with I_0, the use of resistors salvaged from ancient equipment and of unknown manufacture was not considered satisfactory for a serious study. Recently manufactured carbon resistors, which are either of carbon film or of hot-moulded carbon composition, did not exhibit this high-frequency limit in our experiments. It was also not known whether these older resistors had this property due to aging of the carbon or as a consequence of the method of manufacture. A number of attempts at making resistors from chemically etched thin films or carbon deposits, as well as similar attempts with metal films, did not duplicate this property. Finally, a primitive method of making carbon resistors was attempted which consisted of drawing a thick line of india ink on file card stock. The desired response was found with this arrangement. Not only was a high-frequency end to the $1/f$ response observed within a measuring region that was well above the thermal noise, but an unexpected low-frequency switch from a $1/f$ to a $1/f^2$ response was also observed for many samples.

Because of the unusual results found, a detailed description of the fabrication and measuring methods will be given. The resistors were made by slowly drawing multiple overlapping lines of india ink on ordinary $3'' \times 5''$ file card stock which was $0.007''$ thick. It is important that the ink soaks through the file card stock to the other side. This is necessary since if little ink penetration occurs some of the results described here would not be observed because of the reduced cross-sectional area. Also avalanche or popcorn noise would occur due to this low cross-sectional area and consequent high current density. This latter noise source is recognized from the appearance of short irregularly spaced rectangular pulses of roughly 1 to 10 ms duration with amplitudes well above the noise level being observed. This is accompanied by increases in the observed slope of the $1/f$ noise above the usually observed value of ~ 1. Ink penetration was checked by microscopically examining a micro-toned cross section of the resistor. End electrodes were applied using silver print. The india ink used was Rapidgraph© 3080-F†. The measured noise spectra of these resistors were stable over several days but slowly changed, possibly due to crystallization of the carbon, as indicated by a very gradual decrease in the sample resistance.

The noise originating from these resistors was AC coupled, with a time constant of 1 s, to an amplifier consisting of an LM725 and an LM741 wired for an overall gain of 1000. Noise spectrum analysis was performed with a Hewlett-Packard© Model 302A low-frequency wave analyser having a frequency range of 10 Hz to 50 kHz, the output of which was coupled to a Compaq PC. Corrections were made by the computer for the loading of a ten-turn potentiometer used to vary the battery voltage to the sample and a wire-wound series loading resistor of 10 kΩ. The system-generated noise was substantially less than the Nyquist noise for all

† Obtainable from Rotolite Elliot Corporation, Rochester, New York, USA (716-385-1463).

samples for which measurements were made, provided that the resistance of the sample was larger than 5 kΩ.

Numerous checks were made. A probe moved along the samples gave a precisely linear increase of voltage with distance from the electrodes. Measurements at high frequencies (>50 kHz) gave resistance values almost equal to the DC measured value. A sinusoidal wave was injected into the sample through a large resistance while it was connected to the measurement apparatus and gave a flat frequency response. The amplitude response of the measuring system was also exactly linear† over the ranges used. The voltage–current relations of the samples did not show any significant non-linearity with the resistance, changing by <1.5% over the current ranges used. It was positively established that no non-ohmic contacts, capacitive problems, or other significantly unusual behaviour occurred in the samples. In all cases, the samples behaved as ordinary pure resistors within the frequency range used.

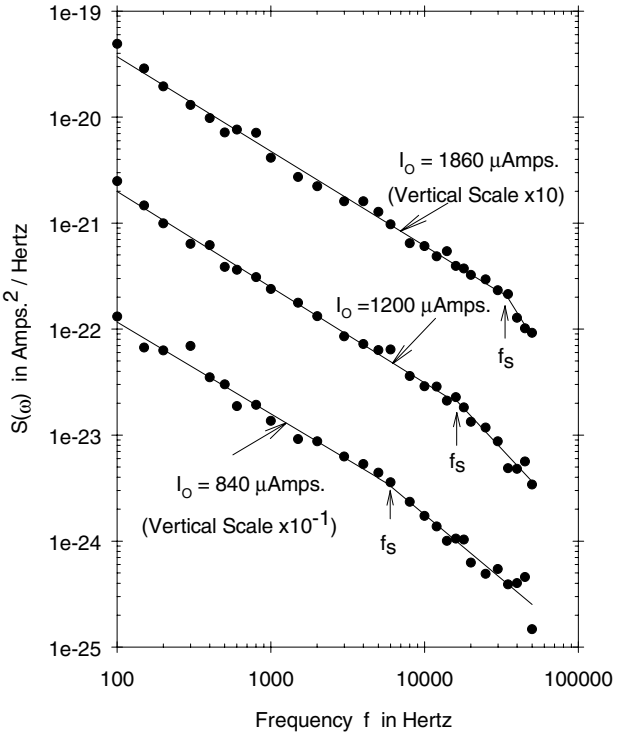

Figure 1. Typical noise spectra of carbon for three applied currents.

The noise spectrums were recorded, averaged, corrected for loading, scaled, and plotted by computer. A typical response is shown in figure 1. The number of readings for each point was 2×10^4 over a period of 10 s. Several background noise power spectra (for $I_0 = 0$) were taken, averaged, and then subtracted from each power spectrum. From the curves taken, the high-frequency cut-off, $f_s = \tau_s^{-1}$, was determined by dividing the data into two files at a trial frequency of f_T, one file with $f < f_T$ and the other for $f > f_T$. Power regressions were separately performed on each file by the computer and then f_T was moved until the point

† The HP 302A Wave Analyzer used has an amplitude non-linearity at output levels below about 2% of the full-scale value shown on the output meter. This problem was circumvented by going to a lower current range when levels below 10% of the full-scale meter reading occurred.

of intersection of the graph of the two power regression lines was at the selected f_T, where $f_s = f_T$. In several cases it was impossible to determine this point, because the slopes of the two sets of data were about equal, and these runs were discarded.

The rather remarkable relation of f_s to I_0 appears in figure 2 and figure 3 for two samples. To show that this result was actual and not caused by some highly random factor in the experiment, the first sample run was repeated three times and nearly the same curve was obtained each time. The second sample run was repeated ten times at each of three different fixed applied currents. The results were that at currents of 840, 1200, and 1860 μA the mean deviations in the measurement of f_s were ± 2.3, ± 2.9, and ± 4.5 kHz respectively. This shows that the variation in individual runs is considerably less than the periodic excursions observed

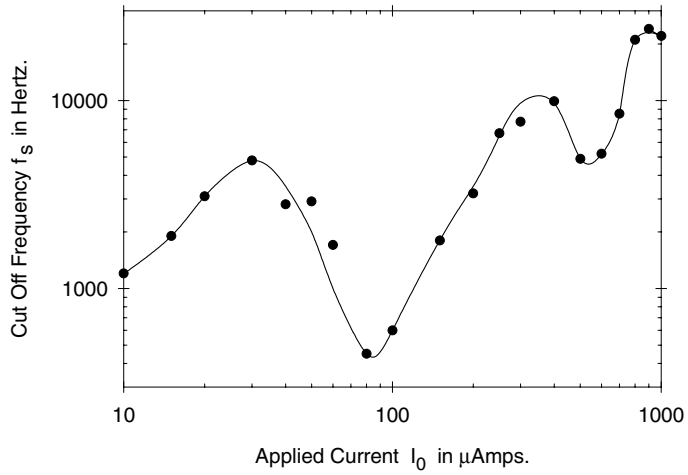

Figure 2. High-frequency cut-off, f_s, versus applied current, I_0; first sample.

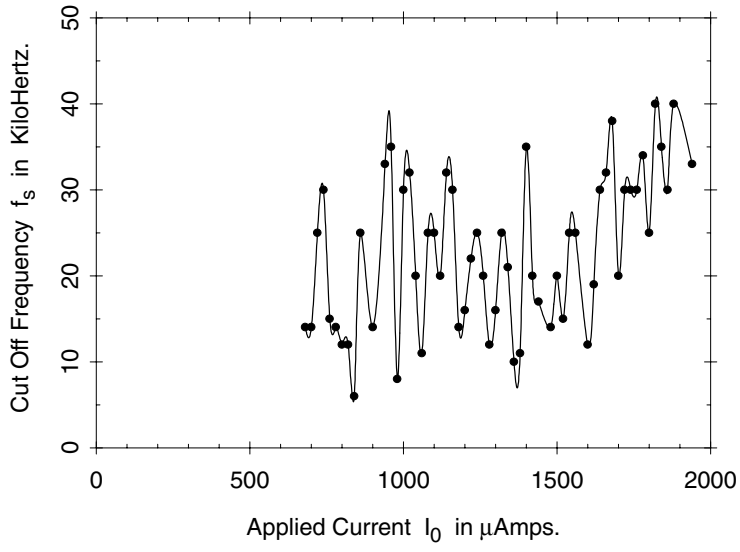

Figure 3. High-frequency cut-off, f_s, versus applied current, I_0; second sample.

in both figures. Consequently, these excursions were determined to be stable, genuine, and repeatable.

The original theory [22] predicted a high-frequency limit, f_s, to the $1/f$ noise power spectrum such that above f_s a $1/f^2$ dependence would be observed. This result was only observed for large values of I_0. At lower values of I_0 the response was obtained to vary from this value as shown in the figures. In addition, the original theory was found to be only valid for resistors of very small cross section. The original theory consequently required further development as well as some modification, which follows.

3. Derivation of noise spectra for a thin conductor and $f < f_s$

First, the noise spectrum of a conductor of small cross section will be considered. This is done so that the effects of thermal flow in the current direction may be neglected as compared with the applied current power flow since the heat flow power is proportional to the area of the cross section. It is proposed that the mass of a defect and its impacted atoms, as it is driven by collisions from conduction electrons causing it to move through the lattice and consequently colliding with and impacting against lattice atoms†, follows the relation

$$m(t) = m_+\left(\frac{x}{a_0 - d} + 1\right)^{\gamma} \tag{3.1}$$

where a_0 is the lattice parameter and d the effective diameter of the lattice atom. This equation would follow from the observation that the impacted mass of a defect or ion that has little or no binding energy, and is moving in a plasma, in a thin fibre, as a sector in a plane, or as a cone in a lattice, would have $\gamma = 0, 1, 2, 3$ respectively. The more rigid the lattice the higher the value of γ, since each impacted atom of the defect would be coupled to additional atoms not adjacent to the impacted mass. In the case of a perfectly inflexible lattice one would expect $\gamma \to \infty$ since each impacted atom would be rigidly coupled to the entire lattice. It is clear that very high values of γ would be found in both metallic and semiconducting solids resulting in extremely slow migration of the defect from its initial position. This removes an objection to the theory as previously given.

Further justification is possible. Let $N = m(t)/m_+$ be the total number of impacted atoms, and $n = 1 + x/(a_0 - d)$ be the number of lattice steps that the defect and its impacted atoms have moved in time t. Then N/n is the average number of atoms that have accumulated in each step. In the next step, ΔN additional atoms will be gained with γ defined as the factor gained above or below this average. Then $\Delta N = \gamma N/n$ which leads to equation (3.1). For very large values of N, γ can be taken as a constant, which is justified since each atom of the impacted mass will not be influenced by impacted atoms many lattice distances apart and, consequently, all impacted atoms are subject to very similar local conditions giving a constant γ.

Conduction electrons collide with the defect and its impacted mass, and leave with the average initial velocity, $V_{init}(t)$, which is equal to the velocity of the defect at that instant. The conduction electrons are assumed to leave instantly, and accelerate to an additional velocity of V_-, after which they travel at a constant average velocity or $V_- + V_{init}$, forming, on average, a rectangular wave pulse during the time of flight. The average values of the energies just before and just after a collision can be equated, giving

$$\frac{1}{2}m_- V_-^2 = \frac{1}{2}m(t)V_{init}^2(t) + \frac{1}{2}m_- V_{init}^2(t). \tag{3.2}$$

† The name 'pluton' has been used for the positively charged defects causing $1/f$ noise while the name 'nepton' has been used for the negative ones. The use of these terms was restricted to point defects occurring in near-perfect lattices.

It is also assumed that between collisions, phonon and, less probably, photon emission reduce the velocity of the defect to a negligible value immediately after each collision. This results in the expression

$$V_{init}(t) = \sqrt{\frac{m_-}{m_+}} V_- \left(\frac{x(t)}{a_0} + 1 \right)^{-\gamma/2} \tag{3.3}$$

where V_- is the average velocity of the colliding conduction electrons and $x(t)$ the displacement in the field direction. A somewhat simplified and perhaps fanciful schematic diagram of this process appears in figure 4. Actually there are many thousands of intervals of τ_c for each τ_s, although only a few are shown. Solving for $V_{init}(t)$ in terms of t gives

$$V_{init}(t) = \sqrt{\frac{m_-}{m_+}} V_- \left(\frac{t}{\tau_s} + 1 \right)^{-\gamma/(2+\gamma)} \tag{3.4}$$

with τ_s defined as

$$\tau_s^{-1} = f_s = \frac{\gamma + 2}{2} \sqrt{\frac{m_-}{m_+}} \frac{V_-}{a_0}. \tag{3.5}$$

The total average current of the sum of the electron current pulses of conduction electrons emitted by ΔN_0 defects during the average lifetimes of these defects, τ_d, which all started at time $t = 0$, is given by

$$i(t) = \frac{I_0 \, \Delta N_0}{N_0} \left[1 + \sqrt{\frac{m_-}{m_+}} \left(\frac{t}{\tau_s} + 1 \right)^{-\gamma/(\gamma+2)} \right] \mathrm{e}^{-t/\tau_d}. \tag{3.6}$$

It should be clear that the average pulse of each individual conduction electron is of constant amplitude since the initial velocity does not change once the electron is emitted, consequently giving a rectangular pulse and not a decaying pulse. However, the ensemble velocity of all the electrons leaving a single defect during the lifetime of the defect decays only because

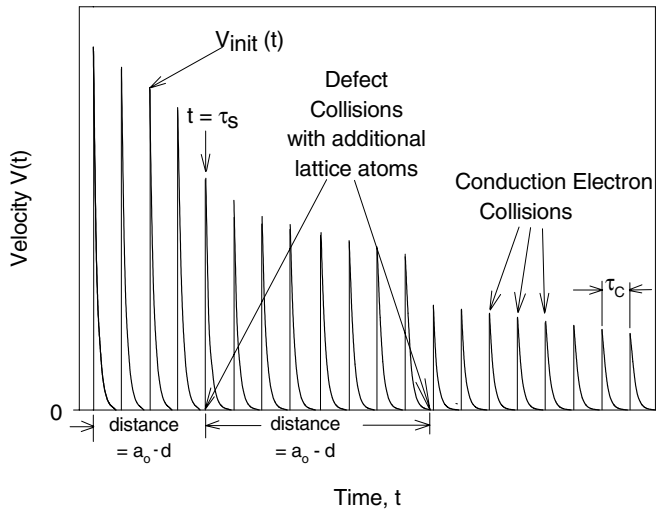

Figure 4. Instantaneous velocity of a defect $V(t)$ versus time. Each peak results from the impact of a conduction electron, where another conduction electron is emitted. The peak velocity, V_{init}, decreases over time because lattice stretching and an additional incremental decrease occur whenever the impacted mass collides with more lattice atoms after moving $a_0 - d$.

each individual conduction electron has a slightly different initial velocity. This decay is very small as compared with the current pulse generated as a consequence of the applied field. The corresponding autocorrelation function, $R(s) = \langle i(t+s)i(t)\rangle$, is given by

$$R(s) = \frac{I_0^2}{N_0}\left[1 + \sqrt{\frac{m_-}{m_+}}\left(\frac{2+\gamma}{2}\right)\left(\frac{s}{\tau_s}+1\right)^{2/(\gamma+2)}\right]e^{-s/\tau_d} \tag{3.7}$$

with the m_-/m_+ term neglected. Using the Wiener–Khintchine theorem

$$S(\omega) = 4\int_0^\infty R(s)\cos(\omega s)\,\mathrm{d}s$$

results in a $1/f$ noise spectrum given by

$$S_\gamma(\omega) = 4\left(\frac{\pi}{2}\right)^{\gamma/(2+\gamma)}\sqrt{\frac{m_-}{m_+}}\frac{I_0^2}{N_0}\frac{(\omega\tau_s)^{-2/(2+\gamma)}}{\omega} \tag{3.8}$$

which is valid in the range $\sqrt{m_+/m_-}\tau_d^{-1} < f < f_s$ and is referred to as the 'gamma' partition. In the case where $\gamma \to \infty$ for a rigid lattice, which would be the case for metallic conductors, this last expression reduces to the Hooge [24] empirical formula:

$$S_\gamma(\omega) = \sqrt{\frac{m_-}{m_+}}\frac{I_0^2}{N_0}\frac{1}{f}. \tag{3.9}$$

An additional component is also generated, which in the range $\tau_d^{-1} < f < \sqrt{m_+/m_-}\tau_d^{-1}$ is greater than the $1/f$ noise, and is the g–r noise of the defect given by

$$S_{\alpha\beta}(\omega) = 4\frac{I_0^2}{N_0}\frac{\tau_d}{(1+\omega\tau_d)^2} \tag{3.10}$$

where τ_d is the shorter of the lifetime and the observation duration for the defect. These various partitions of the noise spectrum are illustrated in figure 5. This derivation is consistent with

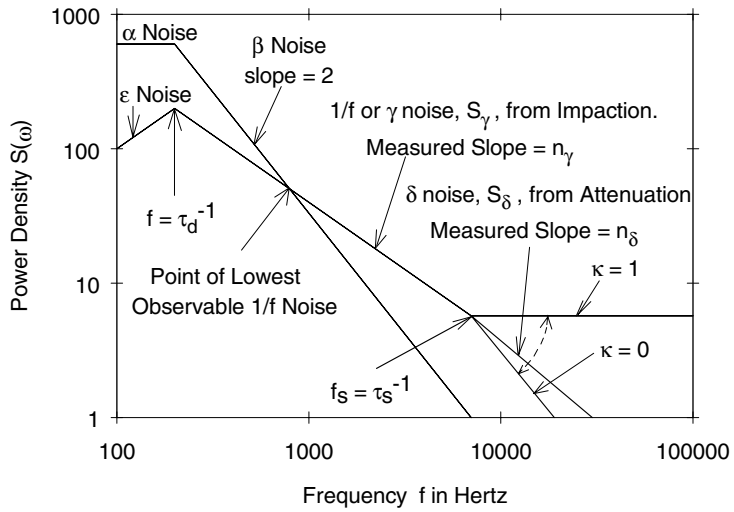

Figure 5. Various partitions of defect noise and their frequency limits. α and β are g–r noise for the defect. γ is the usually observed $1/f$ noise and δ is the region above the cut-off which has a slope of κ. For the damped case, $0 < \kappa < 1$ as shown. ϵ is below α and cannot be easily observed.

the results reported by Voss and Clarke [26] indicating that the resulting $1/f$ noise is due to equilibrium resistance fluctuations and that the process is stationary.

It is noted that equation (3.8) would only allow a frequency dependence between f^{-1} and f^{-2} in the range $\gamma = 0 \rightarrow \infty$. Frequency responses are often observed that are $\sim f^{-0.9}$. This is thought to be the result of two factors. First, it is possible that the striking of the lattice results in a rebound in which the defect actually may move backwards during the lattice collision. This rebounding is a function of the applied current and has been observed in the experiments performed and will be described. Second, this difference is also the result of the current pulses of the conduction electrons which create a noise source that would be flat into the megahertz region and also proportional to current squared. Such a source has been reported [25]. A computer simulation was performed by taking an exact f^{-1} frequency dependence with a random scattering of points and adding a constant equal to the lowest value of this f^{-1} response in an interval of three decades of frequency. This approximated the conditions of the experiments that are reported here. A least-squares fit of the resulting curve gave a response of $f^{-0.8}$. Correcting for background noise would not eliminate this, since this noise source would not appear at $I_0 = 0$.

4. Derivation of noise spectra for $f > f_s$

The origin of the noise spectrum in the region $f > f_s$ depends upon the details of the velocity of the defect within any interval of τ_s. As mentioned previously, noise spectra for the frequency range above f_s are experimentally observed to deviate from a $1/f^2$ dependence, which would be the case for a constant velocity in this time interval. This deviation makes some further theoretical considerations necessary.

The interval between defect lattice collisions is defined as τ_L. It is only in the first interval that $\tau_L = \tau_s$. Thereafter periods that are multiples of τ_s elapse between lattice collisions, as shown in figure 4. First, an expression will be found for V_{init}, the peak velocity after a collision with a conduction electron, and also the velocity at which a conduction electron is emitted, for the case of a negligible applied field and no energy loss due to phonon radiation.

Let t be defined such that $0 < t < \tau_L$ in any interval. Within this interval the defect is bombarded with conduction electrons at average intervals τ_c. After a conduction electron collision, the velocity of the defect, $V(t)$, drops rapidly to a negligible value before the collision with the next conduction electron occurs. The emitted conduction electron is rapidly accelerated by the applied field to a velocity of $V_- + V_{init}$ after which it continues to travel at a constant average velocity. It is this total conduction electron velocity that generates the $1/f$ noise and the rectangular wave shapes observed by Ralls *et al* [20].

In a simplistic view of the lattice, the restoring force, f, for a small displacement of a defect from its initial position, is expressible as $f = kx$ where x is the displacement in the applied field direction. However, for large displacements this is modified and k becomes a variable given by $k = k_0 + k_2x^2 + \cdots$ where x is the displacement from the equilibrium position. The assumption is made—and is verified by the experimental data to be presented—that the defect is in a highly non-linear region of the displacement and consequently that the second term dominates and $k = k_2x^2$. The potential, Φ, of the restoring force is therefore

$$\Phi = \frac{k_2x^4}{4}. \tag{4.1}$$

After each conduction electron collision, the defect travels $\Delta x = a_0$ in time $\Delta t = \tau_c$ and loses

an amount of kinetic energy equal to $\Delta\Phi$. This results in

$$\Delta\Phi = k_2 x^3\,\Delta x = \Delta\left(\frac{1}{2}m_+ V_{init}^2\right) = m_+ V_{init}\,\Delta V_{init} \tag{4.2}$$

and consequently

$$\frac{\Delta V_{init}}{\Delta t} = -2\frac{V_{init}}{t}. \tag{4.3}$$

However, due to phonon and, less probably, photon emission, the defect loses a proportion of this acceleration since the phonon and photon radiations are proportional to the acceleration. Introducing κ, such that $0 < \kappa < 1$, as a unitless transmission factor that modifies the acceleration of the defect for this radiation, consequently gives

$$\frac{\mathrm{d}V_{init}}{\mathrm{d}t} = -2\kappa\frac{V_{init}}{t}. \tag{4.4}$$

This last equation has a solution:

$$V_{init}(t) = V_{init}(0) - Ct^{-2\kappa} \tag{4.5}$$

where C is a constant to be determined which must be consistent with the fact that the average value of $V_{init}(t)$ between two defect lattice collisions is required to be given by equation (3.4).

The wave shapes of equation (3.4) and equation (4.5) both modulate the initial velocity of each conduction electron. The amplitudes of the frequency components of these two quantities both behave as $\sim\sqrt{m_-/m_+}$. The amplitude of the inter-modulation products of these two quantities consequently behave as $\sim m_-/m_+$ with the result that the amplitude of the inter-modulation products are a factor of $\sim\sqrt{m_-/m_+} \approx 10^{-3}$ below the amplitudes of the two levels. This means that the noise spectra generated by equation (3.4) and equation (4.5) interact to a negligible extent, and consequently the frequency spectra may be found from these two expressions independently. It is concluded that finding the autocorrelation function of equation (3.4) and equation (4.5) and applying the Wiener–Khintchine theorem to each separately will produce valid results, with the interaction between them being negligible.

In this derivation, equation (4.5) represents the average wave shape of a single defect while the total wave shape obtained by combining all wave shapes generated consists of τ_d/τ_c groups where each group is, on average, displaced by τ_c in time where τ_d is the lifetime of the defect. There are a total of $N_0\tau_c/\tau_d$ such groups. From this the total noise spectrum generated from equation (4.5) may be found by repeating the previous methods for finding the autocorrelation function and using the Wiener–Khintchine theorem. This results in

$$S_\delta(\omega) = K\frac{(\omega\tau_c)^{2\kappa-1}}{\omega} \tag{4.6}$$

where K is a constant that may be evaluated by equating equation (3.8) and equation (4.6) at the point $f = f_s$. This result is

$$K = 2\pi^{(\gamma-2)/(\gamma+2)}\sqrt{\frac{m_-}{m_+}}\frac{I_0^2}{N_0}(\omega_s\tau_c)^{1-2\kappa} \tag{4.7}$$

with the consequence that

$$S_\delta(\omega) = 2\pi^{(\gamma-2)/(\gamma+2)}\sqrt{\frac{m_-}{m_+}}\frac{I_0^2}{N_0}\left(\frac{\omega}{\omega_s}\right)^{2\kappa-1}\frac{1}{\omega} \tag{4.8}$$

for $f > f_s$.

5. Noise spectrum for a thick conductor and $f < f_s$

Essentially, the current of the conduction electrons is composed of two different components. The first is the current produced by the external field, and is I_0. The second is a current, I_κ, produced by a movement of electrons caused by the thermal energy that can be considered flowing in the material. The Stefan–Boltzmann law gives the radiated thermal energy arriving on any surface of a conducting sample. This thermal energy can be considered to be transferred by conduction electrons, which carry most of this energy, to the opposite surface where it is radiated. Thermal energy arriving on this opposite surface is transferred by the conduction electrons to the initial surface where it is also radiated, resulting in thermal equilibrium. In the direction of the applied current it is possible to partition the conduction electrons at any instant into two macroscopic currents, $I_0 + I_\kappa$ and $-I_\kappa$, resulting is a net thermal current of zero. The $I_0 + I_\kappa$ component generates $1/f$ noise while $-I_\kappa$ does not show a significant noise component in our experiments and it is conjectured that it contributes negligible momentum to the defect due to the interfering effects of the impacted mass. It is only in very thin samples that this thermal flow of the conduction electrons is negligible as compared with the power of the applied current, $I_0^2 R_0$. The power, W, generated by I_κ, is given by the Stefan–Boltzmann law:

$$W = I_\kappa^2 R_0 = \sigma T^4 A \tag{5.1}$$

where A is the cross-sectional area of the sample, σ is the Stefan–Boltzmann constant $=5.67 \times 10^{-8}$ W m^{-2} K^{-4}, and R_0 is the sample resistance.

On the microscopic level each conduction electron carries an initial current of $(I_\kappa + I_0)/N_0$, of which I_0/N_0 is lost on average in a collision. Consequently, neglecting rebounds and resonances,

$$\kappa = \frac{I_\kappa}{I_0 + I_\kappa}. \tag{5.2}$$

The experimentally measured noise power spectrum above f_s is observed to behave as f^{-n_δ}, which defines n_δ. Then, in view of equation (4.8),

$$\kappa = 1 - \frac{n_\delta}{2} \tag{5.3}$$

which results in the expression

$$n_\delta = \frac{2I_0}{I_0 + I_\kappa}. \tag{5.4}$$

It is observed, ignoring resonance effects, that if $I_0 = 0 \to \infty$ then $n_\delta = 0 \to 2$. Other factors can influence these values, as will be discussed.

In the case where $I_0 \gg I_\kappa$ and $\kappa = 0$, the influence of the external field exceeds that of internal thermal effects. In this case the acceleration is negligible and therefore the defect mass moves at a constant average velocity which is what would be expected. In the case where $I_0 = 0$, only the two I_κ-currents exist and only the effects of the thermal motion are observed which, as will be shown, results in a $1/f$ noise source at zero current.

On the basis of the above theory it is apparent that for a sample of thick cross section, the evaluation of the equations of section 3 for $f < f_s$ requires the following obvious modifications. Equation (3.5) becomes

$$f_s = \tau_s^{-1} = \frac{\gamma + 2}{2} \sqrt{\frac{m_-}{m_+}} \frac{\ell(I_0 + I_\kappa)}{e_- N_0 a_0} \tag{5.5}$$

where ℓ is the sample length. Equation (3.8) becomes

$$S_\gamma(\omega) = 4\left(\frac{\pi}{2}\right)^{\gamma/(2+\gamma)} \sqrt{\frac{m_-}{m_+}} \frac{(I_0 + I_\kappa)^2}{N_0} \frac{(\omega\tau_s)^{-2/(2+\gamma)}}{\omega} \tag{5.6}$$

which, for a rigid lattice ($\gamma \to \infty$) and zero current, is

$$S_\gamma(\omega) = \sqrt{\frac{m_-}{m_+}} \frac{I_\kappa^2}{N_0} \frac{1}{f}. \tag{5.7}$$

This last equation is apparently a new type of thermal noise source and is different in characteristics from Nyquist noise. It originates because of the thermal motion of the defects causing a modulation of the initial velocities of the conduction electrons whereas Nyquist noise is the thermal motion of the conduction electrons themselves. The spectral power of this noise for constant resistance varies with the cross-sectional area of the sample and increases with temperature as T^4, while Nyquist noise is constant with cross-sectional area and increases proportionally to T.

6. Resonance phenomena

The experimentally measured functions $f_s(I_0)$, illustrated in figure 2 and figure 3, have what appears to be periodic resonances. Similar periodic resonances also appear in the experimentally measured slopes, n_δ, above f_s, in figure 6 and figure 7. This is qualitatively explained by the idea that when the average frequency of collisions experienced by the conduction electrons, τ_c^{-1}, is equal to the lattice mechanical resonant frequency or a multiple thereof, then an enhancement of the velocity given by equation (4.5) occurs. This gives rise to the apparent resonances that were observed in these figures. Very roughly, if the sample is $\sim$10 mm long and the phonon velocity is $\sim$300 m s^{-1}, then $f \sim 15$ kHz (which is the frequency of the half-wave fundamental mode of sample vibration), which is roughly the value that is observed.

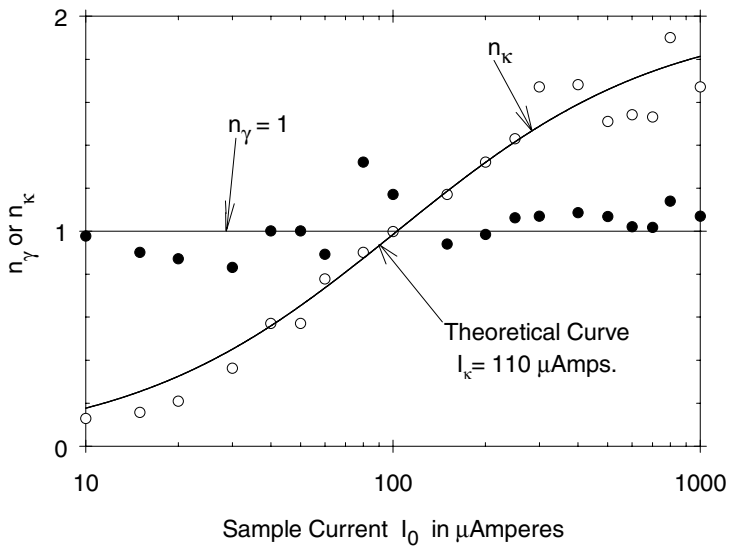

Figure 6. n_γ and n_κ versus applied current I_0; first sample.

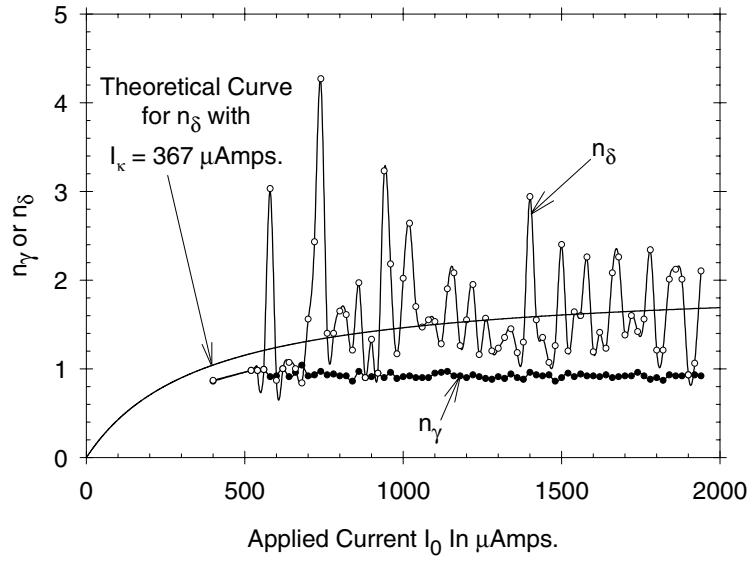

Figure 7. n_γ and n_κ versus applied current I_0; second sample.

It was found that the carbon resistors used all had n_γ about equal to one, as shown in figure 6 and figure 7. In this case γ is large but not infinite; otherwise f_s would not exist, by equation (5.5). This creates numerous resonant frequencies that are activated by the driving force of the bombardment of the conduction electrons and suggests a process that is a kind of emission of conduction electrons stimulated by phonons. It is also noted that in figures 6 and 7 the γ-curves also show small resonances, which indicates that some ringing or bouncing during a lattice collision occurs. This would also contribute to the observed n_γ being somewhat below unity at certain applied currents, as previously discussed.

It should be stressed that the resonances were only seen in the noise generated. At no time did the voltage–current curves or resistance measurements show any sign of these resonances.

7. Experimental results

In figure 6 and figure 7 the experimentally measured values of n_γ and n_δ are shown. The samples were maintained at a temperature of 23 ± 0.5 °C. In these figures, I_κ is always calculated only from the measured resistance, R_0, and the measured dimensions of the samples by using equation (5.1). In figure 6 the value of I_κ was 110 μA, calculated from equation (5.1) using the sample conduction path which was 9 mm long, 4 mm wide, and 0.18 mm thick, with a measured sample resistance $R_0 = 29.0$ kΩ. In figure 7, $I_\kappa = 367$ μA was calculated for a sample that was 9 mm wide, 10 mm long, and 0.18 mm thick, with a measured resistance of $R_0 = 7.1$ kΩ. The theoretical curves produced using these values for I_κ and equation (5.4) have been plotted in both figures, which show good agreement with the theory for the smoothed dampened case.

These results depend heavily on the selection of carbon for the sample. Due to its non-rigidity, its value of γ would be considerably below that found for metals and silicon by using equation (5.5) for the value of f_s. This places f_s at a frequency where the noise is well above the thermal background noise.

Figure 8 shows the data of figure 6 in a linear plot, and the constant $I_\kappa = 110\ \mu$A added to the horizontal axis. The dotted line is the smoothed average of the points and shows that this relation follows the linear dependence of equation (5.5). But it was impossible to determine all the constants of this equation, so the value of the slope of the dotted line could not be claimed as being predicted by this equation, although the linear relation is consistent with the predictions of the theory.

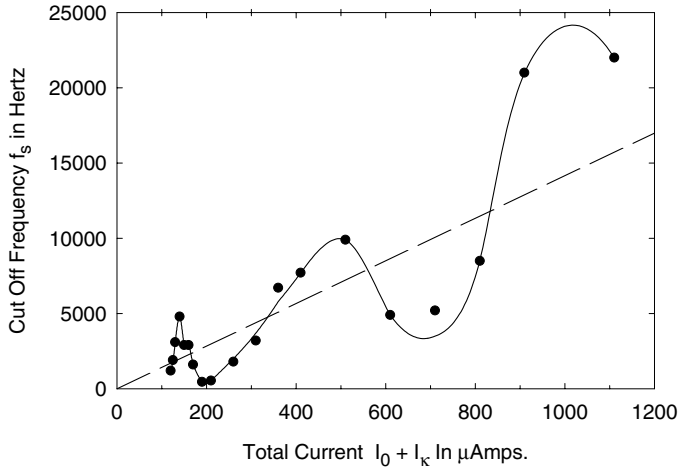

Figure 8. Cut-off frequency, f_s, versus total current, $(I_0 + I_\kappa)$; first sample.

The majority of samples studied showed most of the effects described here. Generally a high-frequency break at some current was found and consequently a value of f_s for the current applied. However, only a few samples showed f_s at a sufficient number of values of the applied currents and at a low enough frequency that curves such as those shown in the figures could be obtained reliably. Attempts at heating the samples for extended times to the point of charring the card stock and also at freezing them did not alter this situation. The most interesting results were obtained with a sample that had aged for three months after being made, which is the sample used in figures 2 and 6, although it is far from certain that aging had anything to do with the results. The sample used in figures 3 and 7 was investigated the day after the sample was made. At this point it is not known what controls these properties. Analysis in a higher frequency range would not help, since this would put the noise to be measured under the thermal background noise. It could be assumed that τ_s is the quantity varying due to variations in the average lattice spacing a_0, but at present this is only a conjecture.

8. Observation of a low-frequency cut-off

A low-frequency end to the $1/f$ dependence was observed for many of the samples with a typical response shown in figure 9. This end point would also vary with the applied current as f_s does. The measured slopes were $n_\beta = 1.76$ and $n_\gamma = 0.90$ as shown. With the estimated slope error of $\approx$0.2 for electron noise, as previously discussed, this would give $n_\beta \approx 1.96$ as compared with its theoretical value of 2.0 and $n_\gamma \approx 1.10$ which is in good agreement with the above theory. From equation (3.8) it is possible to roughly estimate γ for carbon, which for $n_\gamma \approx 1.10$ yields $\gamma \approx 20$. This would place a lower limit on γ for silicon and the metals, which would have values perhaps orders of magnitude higher.

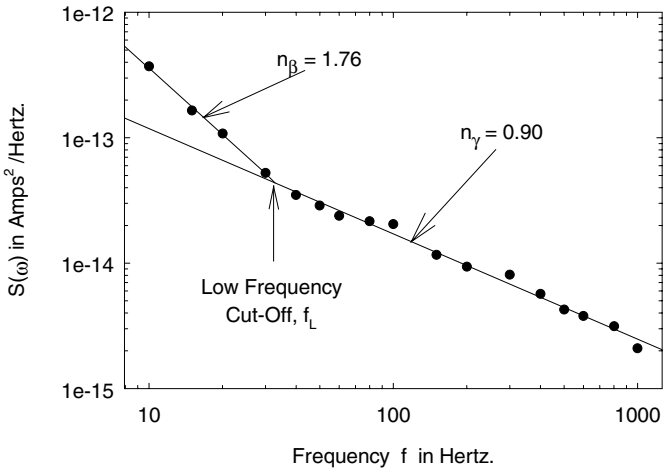

Figure 9. The low-frequency end of the observable $1/f$ noise.

This sample used was cut from the same material as the samples of the other figures but with a conduction path 4 mm long and 4 mm wide. This low-frequency cut-off, f_L, was always observed for samples with conduction paths <4 mm, but not for samples with longer conduction paths. It is evident from this that the observation time for the defect is the limiting factor, and not the lifetime. It is seen that there is a distinct end to the $1/f$ noise, at a theoretical frequency given as $f_L = \pi^{-2}\sqrt{m_+/m_-}\tau_d^{-1} \approx 50\tau_d^{-1}$ for large γ. Although the actual end of the $1/f$ response, which is also the end of the $1/f^2$ response, was not attainable with the present apparatus, it is clear that the end of the *observable* $1/f$ spectrum has been found. The $1/f$ response continues for almost another two decades, but is masked under the g–r noise of the defect as shown in figure 5.

9. Conclusions

The purpose of the present work was to show that f_s varies with the applied current. Not only has this been positively established but also from this work two distinct physical processes have been identified that affect the behaviour of $1/f$ noise in carbon. Below f_s the noise spectrum is determined by the varying mass of the defect due to impaction against lattice atoms, and the assumption of equation (3.1) applied. This equation was shown to be reasonable, and the experimental data fit its predictions well. Above f_s the spectrum was determined by the influence of heat flow, phonon losses, and mechanical vibrations of the lattice, all influencing the initial velocities of conduction electrons and consequently the wave shape of the conduction electrons over the lifetime of the defect. This assumption was mainly contained in equation (4.1) which was also shown to be reasonable, and its consequences fit the data well. These two assumptions were derivable from a very elementary basis similar to that used in considering generation–recombination and thermal noise, which were the original targets of the theoretical study. It is remarkable that the simple view of the conduction process adopted here has been successful in explaining these highly involved phenomena.

Numerous new properties of $1/f$ noise have been reported here which are due to the relatively low γ of carbon as compared with other solids. High values of γ make these properties very difficult to observe. This is probably why they have not been previously

reported for substances with more rigid lattices such as the coordinated metals and the well-known semiconductors, despite the immense amount of work that has been devoted to observing their noise properties. What has not been done is establishing that the mechanism described here is also the source of $1/f$ noise in these other materials; we hope that this will be addressed in future work.

The above theory, after this further verification, may advance the field of noise theory from an area of unsolved problems into an area where noise measurements could provide data about the characteristics of defects unobtainable by other means. It certainly could provide deep insight into the nature of the defects themselves. It is not impossible that this could eventually lead to the discovery of methods for constructing low-defect conductors that operate at room temperature with properties, perhaps, approaching those of a superconductor.

References

[1] Celasco M, Fiorillo F and Mazzetti P 1976 *Phys. Rev. Lett.* **36** 38
[2] Celasco M, Fiorillo F and Mazzetti P 1979 *J. Appl. Phys.* **50** 11
[3] Chen T M, Dieu T P and Moore R D 1985 *IEEE International Reliability Physics Symp.* CH 2113-9/85, p 87
[4] Dagge K, Briggmann J, Reuter C, Seeger A and Stoll H 1996 *AIP Conf. Proc.* **371** 65
[5] Dragge K, Frank W, Seeger A and Stoll H 1996 *Appl. Phys. Lett.* **68** 1198
[6] Feng S, Lee P and Stone A 1986 *Phys. Rev. Lett.* **56** 1960
[7] Fleetwood D and Giordano N 1985 *Phys. Rev.* B **31** 1157
[8] Fleetwood D and Scofield J 1990 *Phys. Rev. Lett.* **64** 579
[9] Fleetwood D, Meisenheimer T and Scofield J 1993 *AIP Conf. Proc.* **285** 339
[10] Gusinski G *et al* 1992 *Sov. Phys.–Solid State* **26** 307
[11] Johnson M and Fleetwood D 1997 *Appl. Phys. Lett.* **70** 1158
[12] Keener C and Weissman M 1991 *Phys. Rev.* B **44** 9178
[13] Koch R H, Lloyd J R and Cronin J 1985 *Phys. Rev. Lett.* **55** 2487
[14] Morozov A and Sigov A 1992 *Sov. Phys.–Solid State* **34** 245
[15] Pelz J, Clarke J and King W 1988 *Phys. Rev.* B **38** 10 371
[16] Potemkin V, Stepanov A and Zhigal'skii G 1993 *AIP Conf. Proc.* **285** 61
[17] Pelz J and Clarke J 1985 *Phys. Rev. Lett.* **55** 738
[18] Pellegrini B 1987 *Phys. Rev.* B **35** 571
[19] Ralls K and Buhrman R 1991 *Phys. Rev.* B **44** 5800
[20] Ralls K, Ralph D and Buhrman R 1989 *Phys. Rev.* B **40** 11 561
[21] Vinokur V and Obukhov S 1989 *Sov. Phys.–JETP* **68** 126
[22] Stephany J F 1998 *J. Appl. Phys.* **83** 3139
[23] Stephany J F 1992 *Phys. Rev.* B **46** 12 175
[24] Hooge F N 1972 *Physica* **60** 130
[25] Hooge F N and Hoppenblouwers A 1969 *Physica* **45** 386
[26] Voss R F and Clarke J 1976 *Phys. Rev.* B **13** 556